Soils and Rocks
An International Journal of Geotechnical and Geoenvironmental Engineering
www.soilsandrocks.com
ISSN 1980-9743
ISSN-e 2675-5475

Case study of Distributed Fiber Optic Sensors (DFOS) in the instrumentation of small-diameter bored piles subjected to tension and compression

Yuri Barbosa[1#], Rodrigo Moraes da Silveira[2], Marcelo Buras[3], Rubens Ramires Sobrinho[4], Marcos Massao Futai[1]

Technical Note

Keywords
Distributed strain sensing
Fibre optic sensors
Electrical strain gauges
Static load test
Bored piles

Abstract

This case study investigates the application of distributed fiber optic sensors for strain monitoring in small-diameter bored piles (D = 0.15 m, L = 3 m) subjected to compressive and tensile loading. A full-scale load test was conducted at the UFPR facilities where, simultaneously, one test pile was loaded in compression and two reaction piles were subjected to tension. The subsurface profile was characterized through a Standard Penetration Test, revealing stiff sandy clay and clayey silt layers. Instrumentation included electrical strain gauges installed at three depths and distributed fiber-optic sensing both in test and reaction piles. The optical fiber of the test pile was pre-tensioned to ensure adequate strain response under compression. Load-displacement curves indicated small settlements and primarily elastic behavior for all piles. For the test pile, comparisons of load transfer profiles derived from strain gauges and fiber optic measurements revealed good agreement at intermediate depths but discrepancies near the pile head and tip, largely attributed to temperature sensitivity and fiber bending effects. Reaction piles showed improved consistency between measurement systems, though early loading stages exhibited spurious negative skin friction in fiber-based results. Overall, the findings confirm the feasibility of using distributed fiber optic sensing in small-diameter bored piles, while highlighting installation-related factors that significantly influence measurement quality.

1. Introduction

Instrumentation based on optical fibers has gained increasing relevance over recent decades, becoming established as a promising technique in a wide range of geotechnical engineering applications, including anchorage systems, slope stabilization, dams, deep foundations, and other structural elements (Hong et al., 2016a). This technique is particularly promising when applied to Distributed Fiber Optic Sensors (DFOS), which, when compared to conventional instrumentation systems, offer a significant set of advantages. These advantages include the ability to continuously monitor strain and temperature along the entire length of a structure, with spatial resolutions on the order of centimeters or even millimeters (Bersan et al., 2018). In addition, fiber optic sensors are characterized by small physical dimensions and low self-weight, immunity to electromagnetic interference, ease of installation, high long-term stability, and the capability of wavelength-division multiplexing, which allows the simultaneous acquisition of a large volume of data through a single interrogation channel (Hong et al., 2016b; Liu et al., 2017; Pelecanos et al., 2018).

In foundation engineering, fiber optic sensing has been widely applied to piles for different purposes, notably the monitoring of the structural integrity of foundation elements (Mohamad et al., 2016; Rui et al., 2017; Kechavarzi et al., 2019; Beddelee et al., 2022; Sun et al., 2022; Sun et al., 2024; Wang et al., 2023), the investigation of load transfer mechanisms between the soil and the pile (Pelecanos et al., 2017; Pelecanos et al., 2018; Bersan et al., 2018; Rui et al., 2021; Felicita et al.,

[#]Corresponding author. E-mail address: yuri.barbosa@usp.br
[1]Universidade de São Paulo, Departamento de Engenharia de Estruturas e Geotécnica, São Paulo, SP, Brasil.
[2]Universidade Federal do Paraná, Departamento de Estruturas Civis, Laboratório de Materiais e Estruturas, Curitiba, PR, Brasil.
[3]Instituto de Tecnologia para o Desenvolvimento, Curitiba, PR, Brasil.
[4]ECS Engenharia Consultoria e Serviços Geotécnicos Ltda, Belo Horizonte, MG, Brasil.

Submitted on March 6, 2026; Final Acceptance on June 27, 2026; Discussion open until May 31, 2027.
Editor: Renato P. Cunha

https://doi.org/10.28927/SR.2027.003426

2024; Chen et al., 2025; Zhou et al., 2025a; Zhou et al., 2025b), the analysis of strain and force distribution profiles along the pile shaft (Monsberger et al., 2016; Seo, 2020), and the assessment of pile dynamic behavior during the driving process (Doherty et al., 2015; Hong et al., 2016b). In addition, this monitoring technique has been applied in the identification of defects associated with the construction process of bored piles, such as geometric variations and structural discontinuities (Pelecanos et al., 2017; Beddelee et al., 2022).

Despite the widespread adoption of fiber optic instrumentation in foundation engineering, relevant gaps remain regarding the exploration of its full potential in specific applications. Among these, the evaluation of the mechanical behavior of the same pile type installed at the same site but subjected to different types of loading stands out. Accordingly, this study aims to present the results of DFOS-based instrumentation applied to three small-diameter bored piles (D = 0.15 m, L = 3 m) installed in Curitiba, Paraná State, Brazil. One pile was subjected to compressive loading, while the other two were loaded in tension, as they were part of the reaction system for the compression test. For all piles, the strains measured by the distributed optical fiber were compared with those obtained from conventional strain gauges. This instrumentation technology has not yet been applied in this manner in Brazil, and the present research is part of an initial experimental campaign; therefore, the piles have relatively small dimensions. The outcomes of this study are intended to support future applications of DFOS instrumentation in full-scale foundation elements.

2. Materials and methods

The location selected for conducting the load test is within the facilities of Instituto de Tecnologia para o Desenvolvimento (LACTEC) and Universidade Federal do Paraná (UFPR), in Curitiba, Paraná State. A Standard Penetration Test (SPT) was performed to characterize the subsurface conditions, and the results are presented in Figure 1. The soil profile is characterized by a surface layer of crushed stone and gravel, followed by a layer of sandy clay

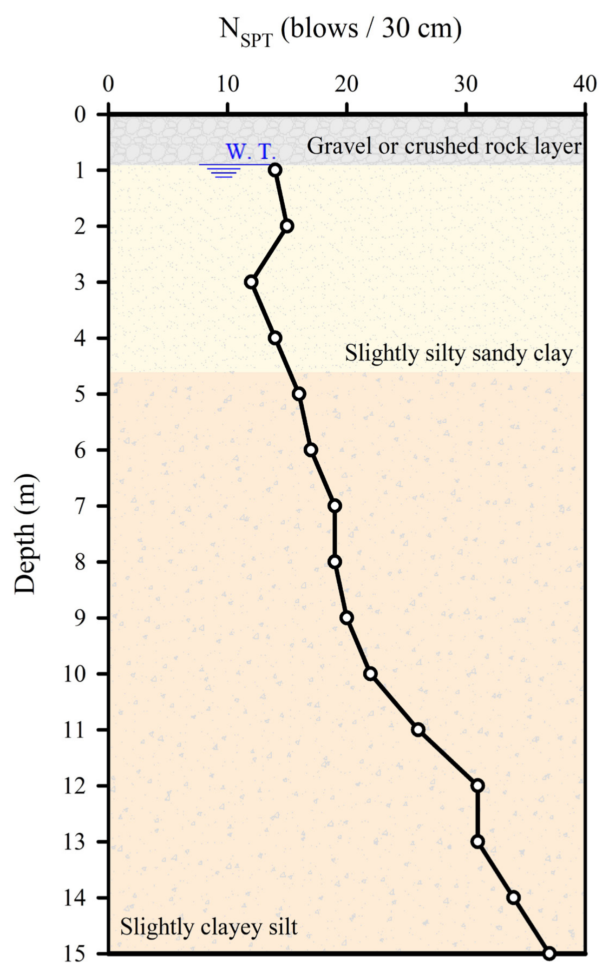

Figure 1. Subsurface profile from the SPT test.

and another of clayey silt, all exhibiting stiff to very stiff and competent behavior ($N_{SPT} > 10$). The groundwater level was encountered at approximately 1 m depth. The groundwater table was not encountered during the 3 m pile excavation because it was carried out during the dry season.

The load test setup began with the preparation of the instrumentation using strain gauges and DFOS. The first consisted of installing diametrically opposed pairs of electrical strain gauges configured in a full-bridge arrangement along the central reinforcement bars of each pile (test pile and both reaction piles) at the target depths for measurement (0.5, 1.5, and 2.8 m below the top of the bars after installation). The DFOS, in turn, was bonded along the entire length of the central reinforcement bars of all three piles. To prevent sharp bends in the optical fiber at the bar tips, pulleys were installed to ensure proper signal quality in that region (Figure 2-a). Once the central tie rods were installed within the borehole, the optical fiber of the test pile was pre-tensioned using a system consisting of a metallic housing (Figure 2-b), steel plates designed to secure the fiber without causing damage, and a set of metal rods and a valve assembly that enabled fiber tensioning through valve rotation. Because the fiber cannot be effectively compressed, it is necessary to apply an initial pre-tension so that the reduction of this tensile strain can be recorded and interpreted as compressive strain in the segment where the fiber was installed. The pre-tensioning process was applied exclusively to the fiber of the test pile (Mohamad et al., 2015; Hong et al., 2016b; Bersan et al., 2018; Pelecanos et al., 2018; Kania et al., 2020), and was applied to approximately 0.1% strain relative to the 3 m length of the test pile, corresponding to about 3000 με.

The overall setup of the static load test comprised, in addition to the compression test pile, two reaction piles subjected to tension, a reaction beam, and steel wedges (Figure 2-c). The pile concreting was performed three days before the load test, made possible by adopting a minimum compressive strength (f_{ck}) of 30 MPa for this same period. A superplasticizer additive, Sika ViscoCrete – 6090 HN, was also used to reduce the water content in the mixture while maintaining the required workability, corresponding to a slump of 150 mm. After concreting, three cylindrical specimens with dimensions of 10 × 20 cm were molded for the determination of the modulus of elasticity, with an average value of 33.1 GPa obtained. All three piles had

Figure 2. Experimental setup of the fiber optic instrumentation and static load test: (a) pulley at the pile tip, (b) system for fiber pre-tensioning, (c) general assembly of the static load test, (d) detail of the test pile head – load cell and hydraulic jack, (e) data acquisition system, and (f) DSTS OzOptics interrogator.

a final diameter of 0.15 m and a length of 3 m, spaced approximately 0.83 m apart from each other.

The load test was carried out according to the quick-maintained load procedure described in NBR 16903 (ABNT, 2020). At the head of the test pile, a hydraulic jack and a load cell were positioned for load application and measurement, respectively (Figure 2-d). Three LVDTs (Linear Variable Differential Transformer) at the head of the test pile and a digital deflectometer on each reaction pile were also installed for displacement measurements. The decision to use three LVDTs at the head of the test pile, rather than four as recommended by NBR 16903 (ABNT, 2020), was due to space limitations that prevented the installation of a fourth displacement measuring device and is consistent with the requirements of ASTM D1143/D1143M-20 (ASTM, 2020) for small-diameter piles. The measurements of applied load from the load cell, displacements from the LVDTs, and specific strains from the strain gauges were acquired using the HBM QuantumX Assistant data acquisition system (Figure 2-e), together with the Catman Easy software. The DSTS (Distributed Strain and Temperature Sensors) interrogator from OzOptics was employed for specific strain measurements of the optical fiber (Figure 2-f) and the Brillouin Optical Time-Domain Analysis (BOTDA) module was used to acquire strain measurements at 8 cm intervals along the fiber. The principles of fiber optic strain sensing are presented in Silveira et al. (2025) and Seo (2020), while its applications in BOTDA can be found in Liu et al. (2017) and Kechavarzi et al. (2019). Table 1 presents the configurations used in the DSTS interrogator for the load test. The fiber employed is supplied by Sensornet, with strain coefficient (C_ε) of 19.38 με/MHz. Further information about the fiber and the calibration methodology can be found in Silveira et al. (2025).

3. Analysis and results

3.1 Load-displacement results

Figure 3 shows the load–settlement curves for the test pile and the reaction piles. From the figure, it can be observed that the maximum displacements reached were approximately 0.80 mm and 0.30 mm for the test and reaction piles, respectively, values far below 15 mm (corresponding to 10% of the pile diameter). After unloading, the test pile

Table 1. DSTS interrogator configuration for the load test.

Parameter	Value
Pulse width (ns)	10
Input range	1V
Spatial step (m)	0.08
Process method	Fast General Analysis
Average number	1000
Frequency step (MHz)	5

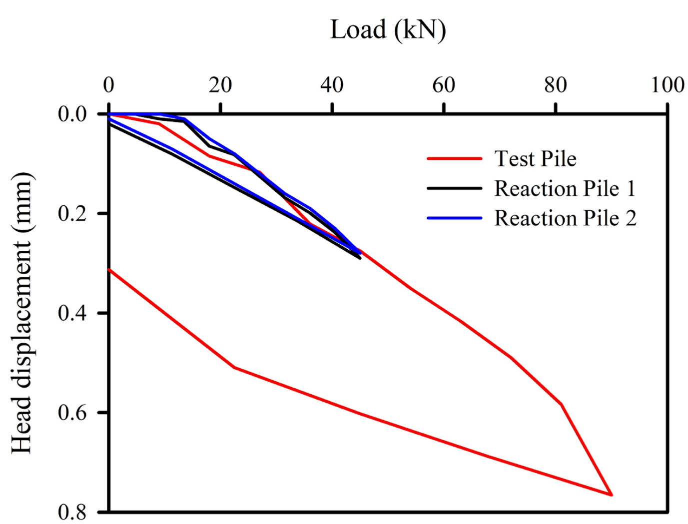

Figure 3. Load–settlement curves of the test pile and both reaction piles.

exhibited a residual displacement of about 0.3 mm, while both reaction piles returned to nearly zero displacement, indicating an almost fully elastic behavior.

3.2 Load along depth

Figure 4 shows the frequency measured along the fiber length before and at the final loading stage of the static load test. The section corresponding to the test pile was approximately between 52 and 58 m, while for reaction piles 1 and 2, the sections were between 40 and 46 m and 65 and 71 m, respectively. The 6 m length for each pile corresponds to 3 m of fiber in the downward direction and 3 m in the upward direction within each pile, consistent with their actual lengths. From Figure 4, the higher frequency observed in the interval corresponding to the test pile is due to the pre-tensioning applied after the static load test. In the fiber sections outside the piles, the largest frequency variations are due to sun exposure and ambient temperature changes, factors that also affect the fiber strain (Bersan et al., 2018).

According to Hong et al. (2016b), the basic relationship between the light frequency v and strain ε is given by Equation 1 as follows:

$$v(\varepsilon) = v_0 \cdot (1 + C_\varepsilon \cdot \varepsilon) \quad (1)$$

where $v(\varepsilon)$ is the Brillouin scattering frequency generated by strain change, v_0 is the reference frequency, and C_ε is the constant strain coefficient calibrated. Thus, given two frequency measurements and the known deformation coefficient, the specific strain can be estimated and, consequently, the axial force F applied at any section i can be determined according to Equation 2:

$$F_i = E_p \cdot \varepsilon_i \cdot A_p \quad (2)$$

in which E_p and A_p are the elastic modulus and the cross-sectional area of the pile.

Figure 5 illustrates the comparison of load distributions along the pile depth, as interpreted from strain measurements obtained using electrical strain gauges and distributed fiber-optic sensors. In the case of the fiber-optic data, both downward and upward measurements, as well as their averaged profile, are presented. The results reveal notable discrepancies between the fiber-optic and strain-gauge results, mainly within the upper 1.20 m and near the pile tip. For the 90 kN loading stage, the maximum average load obtained from the DFOS measurements was 290 kN at a depth of 0.42 m. At the depth corresponding to the first strain gauge level (0.50 m), the load estimated by the DFOS was 200 kN, which is 110 kN higher. At the pile tip, the load measured by the strain gauge was 48 kN, whereas the DFOS estimated a load of 80 kN, representing a value approximately 67% higher.

The first difference can be attributed to the higher sensitivity of this fiber segment to ambient temperature variations (Bersan et al., 2018; Kania et al., 2020). Another possible factor is the proximity to the load application point or the sharp bending of the fiber near the pile head. At the pile tip, the use of a pulley intended to prevent excessive bending did not perform as expected, as the fiber-optic data suggest an apparent load increase in that region, indicating negative skin friction, an interpretation inconsistent with the actual load-transfer mechanism. Conversely, at intermediate depths,

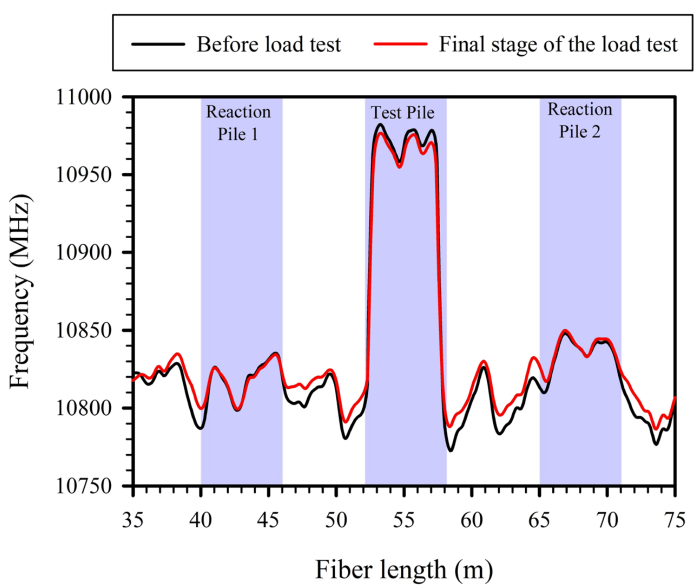

Figure 4. Comparison of frequency profiles along the optical fiber before and at the final loading stage of the static load test.

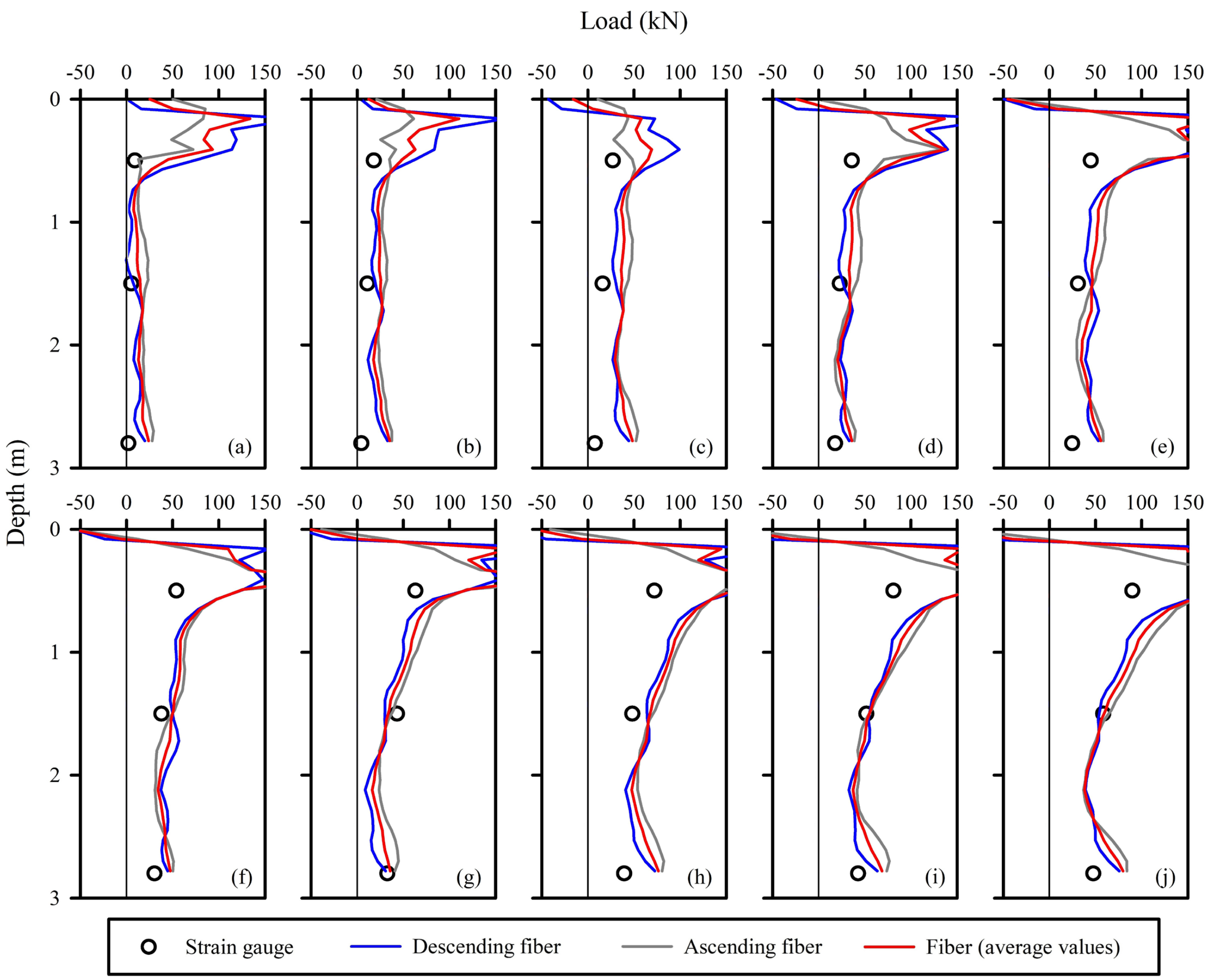

Figure 5. Comparison between strain gauges and optical fiber measurements for load along depth of the test pile in every loading stage: (a) 9 kN, (b) 18 kN, (c) 27 kN, (d) 26 kN, (e) 45 kN, (f) 54 kN, (g) 63 kN, (h) 72 kN, (i) 81 kN, and (j) 90 kN.

both measurement systems yielded comparable results, and the upward and downward fiber readings exhibited minimal variation for depths greater than 0.80 m.

Figure 6 presents the results for Reaction Pile 1, which was subjected to tensile loading. The strain gauge instrumentation indicated that the entire applied load was resisted between depths of approximately 0.5 and 1.5 m, as no load development was observed at the second and third instrumented levels. Regarding the values obtained from the fiber optic measurements, it can be observed that the results were inconsistent with those from the strain gauges during the first three loading stages, as they indicated negative loads along the entire length below 0.5 m. Between the fourth and seventh loading stages, the fiber optic readings became consistent with the three strain-gauge-instrumented levels, although negative loads were still observed between the first and second levels. This behavior ceased to occur from the seventh stage onward.

Figure 7 presents the results for Reaction Pile 2, which was also subjected to tensile loading. In this pile, the strain gauge at the 1.5 m level was not functional. For the remaining two instrumented levels, the load values obtained from both the fiber optic and strain gauge measurements converged throughout all loading stages. However, regarding the mechanical behavior between depths of 0.5 and 1.2 m, the fiber optic data indicated increasing load values with depth during the first three loading stages, suggesting the mobilization of negative skin friction in this region, an outcome that does not correspond to the actual behavior. From this stage onward, the increase in load along this interval became consistent with the expected response. Unlike the previous case, Reaction Pile 2 exhibited load development between the instrumented levels at 0.5 and 2.8 m, with the load being fully dissipated near the latter depth. Furthermore, the variation between the ascending and descending fiber optic readings was smaller in this case than that observed for Reaction Pile 1.

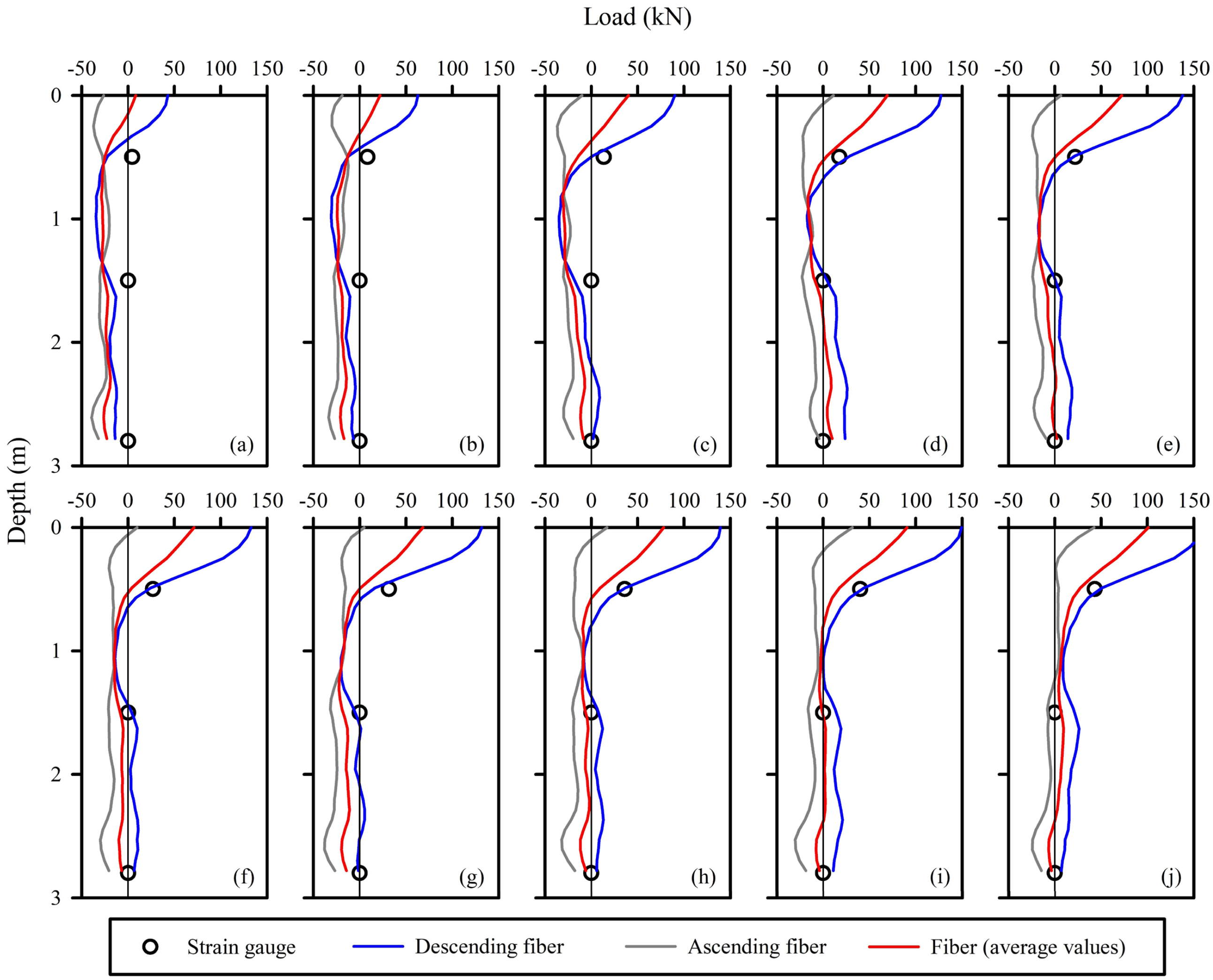

Figure 6. Comparison between strain gauges and optical fiber measurements for load along depth of the reaction pile 1 in every loading stage: (a) 4.5 kN, (b) 9 kN, (c) 13.5 kN, (d) 18 kN, (e) 22.5 kN, (f) 27 kN, (g) 31.5 kN, (h) 36 kN, (i) 40.5 kN, and (j) 45 kN.

4. Conclusion

The present case study demonstrated that distributed fiber optic sensors can effectively capture load transfer mechanisms in small-diameter bored piles. For the compression pile, the agreement between DFOS and strain-gauge measurements was generally satisfactory at intermediate depths. However, discrepancies were observed near the pile head and pile tip, where the fiber-optic measurements exhibited localized anomalies and larger deviations from the conventional instrumentation. For the reaction piles subjected to tension, the consistency between DFOS and strain-gauge measurements improved as the applied load increased although anomalous load distributions were observed during the initial loading stages. Potential effects associated with shallow soil temperature variations and pre-tension should be regarded as hypotheses rather than confirmed influencing factors, once temperature measurements were not taken during the monitoring period and the pre-tension level was considered constant along the length of the compression pile. The results also indicate that installation-related aspects may significantly affect measurement quality, particularly in regions where the optical fiber is subjected to influence of the load application point, geometric discontinuities, influence of external factors, anchorage details, or abrupt changes in direction. Additional investigation is required to quantify the influence of these factors on the measured strain profiles.

The conclusions of this work are limited to the tested configuration, and future research should include additional field tests under different geotechnical conditions, instrumentation layouts, and pile geometries. Furthermore, a comprehensive parametric finite element study, calibrated and validated using the experimental measurements, is recommended to evaluate the influence of installation details and soil-pile interaction mechanisms on DFOS measurements.

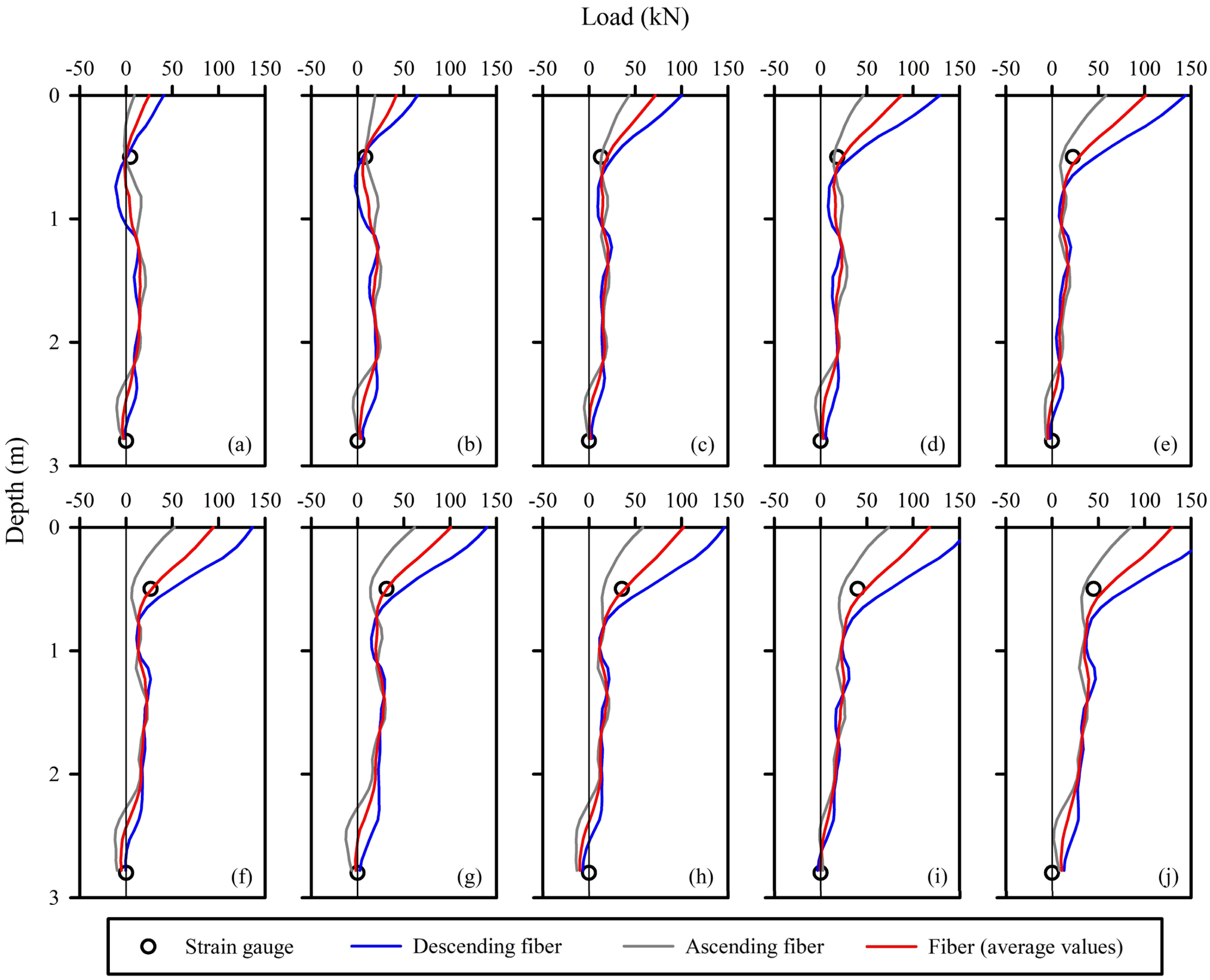

Figure 7. Comparison between strain gauges and optical fiber measurements for load along depth of the reaction pile 2 in every loading stage: (a) 4.5 kN, (b) 9 kN, (c) 13.5 kN, (d) 18 kN, (e) 22.5 kN, (f) 27 kN, (g) 31.5 kN, (h) 36 kN, (i) 40.5 kN, and (j) 45 kN.

Acknowledgements

The authors would like to thank UFPR and LACTEC for providing the facilities for the field test. The authors also acknowledge LACTEC for the technical support, the National Council for Scientific and Technological Development (CNPq) through grant 306379/2021-0, and the Cátedra Under Rail – VALE Project for providing the research scholarships.

Declaration of interest

The authors have no conflicts of interest to declare. All co-authors have observed and affirmed the contents of the paper and there is no financial interest to report.

Authors' contributions

Yuri Barbosa: formal analysis, investigation, visualization, writing – original draft. Rodrigo Moraes da Silveira: conceptualization, formal analysis, investigation, methodology, writing – review & editing. Marcelo Buras: investigation, methodology, validation. Rubens Ramires Sobrinho: formal analysis, investigation, validation. Marcos Massao Futai: funding acquisition, project administration, resources, supervision.

Data availability

The datasets generated analyzed in the course of the current study are available from the corresponding author upon request.

Declaration of use of generative artificial intelligence

This work was prepared without the assistance of any generative artificial intelligence (GenAI) tools or services. All aspects of the manuscript were developed solely by the

authors, who take full responsibility for the content of this publication.

List of symbols and abbreviations

f_{ck}	Characteristic compressive strength of concrete
A_p	Cross-sectional area of the pile
BOTDA	Brillouin Optical Time-Domain Analysis
C_ε	Strain coefficient of the fiber
D	Pile diameter
E_p	Elastic modulus of the pile
F	Force applied in a section
DFOS	Distributed Fiber Optical Sensing
DSTS	Distributed Strain and Temperature Sensors
L	Pile length
LACTEC	Instituto de Tecnologia para o Desenvolvimento
LVDT	Linear Variable Differential Transformer
N_{SPT}	Number of blows for the last 30 cm of SPT penetration
SPT	Standard Penetration Test
UFPR	Universidade Federal do Paraná
ε	Specific strain
v	Brillouin scattering frequency
v_0	Reference frequency

References

ABNT NBR 16903. (2020). *Soil – Static load test on deep foundation*. ABNT - Associação Brasileira de Normas Técnicas, Rio de Janeiro, RJ (in Portuguese).

ASTM D1143/D1143-20. (2020). *Standard test methods for deep foundations under static axial compressive load*. ASTM - American Society for Testing and Materials, West Conshohocken, PA.

Beddelee, A.A.A.M., Mohamad, H., & Tee, B.P. (2022). Validation on laboratory simulated optical fibre sensor instrumented bored pile defect using 3D Finite Element Method. *Journal of Civil Structural Health Monitoring*, 12(5), 991-1007. https://doi.org/10.1007/s13349-022-00588-y.

Bersan, S., Bergamo, O., Palmieri, L., Schenato, L., & Simonini, P. (2018). Distributed strain measurements in a CFA pile using high spatial resolution fibre optic sensors. *Engineering Structures*, 160, 554-565. https://doi.org/10.1016/j.engstruct.2018.01.046.

Chen, Y., Tian, Z.G., Huang, M.L., Gao, Y.L., Wu, Y.J., & Yan, G.H. (2025). Field application of BOFDA-based distributed fiber optic sensing in static load testing of cast-in-place pile foundations. *Frontiers in Built Environment*, 11, 1700987. https://doi.org/10.3389/fbuil.2025.1700987.

Doherty, P., Igoe, D., Murphy, G., Gavin, K., Preston, J., McAvoy, C., & Skov Gretlund, J. (2015). Field validation of fibre Bragg grating sensors for measuring strain on driven steel piles. *Géotechnique Letters*, 5(2), 74-79. https://doi.org/10.1680/geolett.14.00120.

Felicita, M., Pagella, G., Ravenshorst, G., Mirra, M., & van de Kuilen, J.W. (2024). Assessment of in-situ stress distribution and mechanical properties of wooden foundation piles instrumented with distributed fiber optic sensors (DFOS). *Case Studies in Construction Materials*, 20, e03139. https://doi.org/10.1016/j.cscm.2024.e03139.

Hong, C.Y., Zhang, Y.F., Zhang, M.X., Leung, L.M.G., & Liu, L.Q. (2016a). Application of FBG sensors for geotechnical health monitoring, a review of sensor design, implementation methods and packaging techniques. *Sensors and Actuators. A, Physical*, 244, 184-197. https://doi.org/10.1016/j.sna.2016.04.033.

Hong, C.Y., Zhang, Y.F., & Liu, L.Q. (2016b). Application of distributed optical fiber sensor for monitoring the mechanical performance of a driven pile. *Measurement : Journal of the International Measurement Confederation*, 88, 186-193. https://doi.org/10.1016/j.measurement.2016.03.052.

Kania, J.G., Sorensen, K.K., & Fellenius, B.H. (2020). Application of distributed fibre optic cables in piles. *Geotechnical Engineering Journal of the SEAGS & AGSSEA*, 51(1), 94-102. https://doi.org/10.14456/seagj.2020.69.

Kechavarzi, C., Pelecanos, L., De Battista, N., & Soga, K. (2019). Distributed fibre optic sensing for monitoring reinforced concrete piles. *Geotechnical Engineering Journal of the SEAGS & AGSSEA*, 50(2), 43-51. https://doi.org/10.14456/seagj.2019.40.

Liu, B., Zhang, D., & Xi, P. (2017). Mechanical behaviors of SD and CFA piles using BOTDA-based fiber optic sensor system: A comparative field test study. *Measurement : Journal of the International Measurement Confederation*, 104, 253-262. https://doi.org/10.1016/j.measurement.2017.03.038.

Mohamad, H., Kueh, A.B.H., & Rashid, A.S.A. (2015). Distributed optical-fibre strain sensing in reinforced concrete structures. *Jurnal Teknologi*, 74(4), 93-97. https://doi.org/10.11113/jt.v74.4615.

Mohamad, H., Tee, B.P., Ang, K.A., & Chong, M.F. (2016). Characterizing anomalies in distributed strain measurements of cast-in-situ bored piles. *Jurnal Teknologi*, 78(8-5), 75-82. https://doi.org/10.11113/jt.v78.9626.

Monsberger, C., Woschitz, H., & Hayden, M. (2016). Deformation measurement of a driven pile using distributed fibre-optic sensing. *Journal of Applied Geodesy*, 10(1), 61-69. https://doi.org/10.1515/jag-2015-0021.

Pelecanos, L., Soga, K., Chunge, M.P., Ouyang, Y., Kwan, V., Kechavarzi, C., & Nicholson, D. (2017). Distributed fibre-optic monitoring of an Osterberg-cell pile test in London. *Géotechnique Letters*, 7(2), 152-160. https://doi.org/10.1680/jgele.16.00081.

Pelecanos, L., Soga, K., Elshafie, M.Z., Battista, N., Kechavarzi, C., Gue, C.Y., Ouyang, Y., & Seo, H.J. (2018). Distributed fiber optic sensing of axially loaded bored piles. *Journal of Geotechnical and Geoenvironmental*

Engineering, 144(3), 04017122. https://doi.org/10.1061/(ASCE)GT.1943-5606.0001843.

Rui, Y., De Battista, N., Kechavarzi, C., Xu, X., & Yin, M. (2021). Distributed fiber optic monitoring of a CFA pile with a central reinforcement bar bundle. *Frontiers of Structural and Civil Engineering*, 15(1), 167-176. https://doi.org/10.1007/s11709-020-0581-z.

Rui, Y., Kechavarzi, C., O'Leary, F., Barker, C., Nicholson, D., & Soga, K. (2017). Integrity testing of pile cover using distributed fibre optic sensing. *Sensors*, 17(12), 2949. https://doi.org/10.3390/s17122949.

Silveira, R.M., Buras, M., Pereira Filho, A.L.D., Fernandes, J.F., & Futai, M.M. (2025). Laboratory tests using distributed fiber optical sensors for strain monitoring. *Sensors*, 25(2), 324. https://doi.org/10.3390/s25020324.

Seo, H. (2020). Monitoring of CFA pile test using three dimensional laser scanning and distributed fiber optic sensors. *Optics and Lasers in Engineering*, 130, 106089. https://doi.org/10.1016/j.optlaseng.2020.106089.

Sun, Q., Elshafie, M.Z., Barker, C., Fisher, A., Schooling, J., & Rui, Y. (2022). Integrity monitoring of cast in-situ piles using thermal approach: A field case study. *Engineering Structures*, 272, 114586. https://doi.org/10.1016/j.engstruct.2022.114586.

Sun, Q., Elshafie, M.Z., Xu, X., & Schooling, J. (2024). Pile defect assessment using distributed temperature sensing: fundamental questions examined. *Structural Health Monitoring*, 23(3), 1701-1724. https://doi.org/10.1177/14759217231189426.

Wang, J., Zhu, H., Tan, D., Li, Z., Li, J., Wei, C., & Shi, B. (2023). Thermal integrity profiling of cast-in-situ piles in sand using fiber-optic distributed temperature sensing. *Journal of Rock Mechanics and Geotechnical Engineering*, 15(12), 3244-3255. https://doi.org/10.1016/j.jrmge.2023.02.028.

Zhou, J.J., Zhang, R.H., Yu, J.L., Gong, X.N., & Ming, W. (2025a). Field study on the shaft capacity of pre-bored grouted planted pile embedded in deep soft soil. *Acta Geotechnica*, 20(4), 1935-1946. https://doi.org/10.1007/s11440-024-02522-6.

Zhou, J., Zhang, R., Gong, X., Yu, J., & Yan, T. (2025b). Field tests on compressive bearing capacity of cast-in-situ pile and pre-bored grouted PHC pile. *Journal of Rock Mechanics and Geotechnical Engineering*, https://doi.org/10.1016/j.jrmge.2025.08.032.